

# The chromium dimer: closing a chapter of quantum chemistry

Henrik R. Larsson,<sup>\*,†,‡</sup> Huanchen Zhai,<sup>†</sup> C. J. Umrigar,<sup>¶</sup> and Garnet Kin-Lic Chan<sup>\*,†</sup>

<sup>†</sup>*Division of Chemistry and Chemical Engineering, California Institute of Technology, Pasadena, CA 91125, USA*

<sup>‡</sup>*Department of Chemistry and Biochemistry, University of California, Merced, CA 95343, USA*

<sup>¶</sup>*Laboratory of Atomic and Solid State Physics, Cornell University, Ithaca, NY 14853, USA*

Received August 26, 2022; E-mail: larsson22\_cr2[at]larsson-research.de; garnetc[at]caltech.edu

---

**Abstract:** The complex electronic structure and unusual potential energy curve of the chromium dimer have fascinated scientists for decades, with agreement between theory and experiment so far elusive. Here, we present a new ab initio simulation of the potential energy curve and vibrational spectrum that significantly improves on all earlier estimates. Our data support a shift in earlier experimental assignments of a cluster of vibrational frequencies by one quantum number. The new vibrational assignment yields an experimentally derived potential energy curve in quantitative agreement with theory across all bond lengths and across all measured frequencies. By solving this long-standing problem, our results raise the possibility of quantitative quantum chemical modeling of transition metal clusters with spectroscopic accuracy.

---

Transition metal chemistry plays a pivotal role in catalysis, biochemistry, and the energy sciences, but the complex electronic structure of the *d*-shells challenges our modeling and understanding of such processes.<sup>1–3</sup> Amongst the most complicated of small transition metal molecules is the chromium dimer, often described as a grand challenge problem of small molecule quantum chemistry, and whose unusual bonding and potential energy curve (PEC) has puzzled scientists for decades.<sup>4–15,21,22</sup> Addressing this is relevant for other dichromium compounds, as well as for other compounds where multiple metal-metal bonds and spin coupling appear.<sup>1–5,7,9,14,16–19</sup> The Cr–Cr bond in the bare dimer is a formal sextuple bond, and when complexed with ligands, was the first example of a quintuple bond.<sup>16,20</sup> Although the formal bond order is high, the PEC inferred from photoelectron spectroscopy indicates a short and weak bond with a narrow minimum around 1.68 Å, and an extended shelf at around 2.5 Å.<sup>11</sup> The curve takes this form because the Cr 4s and 3d atomic orbitals are of very different size, with the minimum corresponding mostly to 3d orbital interactions and the shelf to 4s orbital interactions. Beyond this picture, a quantitative understanding remains lacking. In particular, theoretical predictions of the binding curve deviate substantially from the experimentally derived curve, as well as from each other, while the experimental curve is uncertain at longer bond lengths. Here we show that a combined analysis from new numerical simulations using state-of-the-art quantum chemistry methods, together with existing experimental data, yields a definitive picture of the Cr<sub>2</sub> PEC. In particular, our work suggests a reassignment of the vibrational subbands in the shelf region, bringing theory and experiment finally into quantitative agreement.

The complex electronic structure arises from the interplay of two types of electron correlation. First, there is the

spin-coupling of the 12 valence electrons in the 3d and 4s Cr atoms shells; this is termed static correlation. Because the many-electron wavefunction of the valence electrons is not well captured by a single determinant, we refer to the electronic structure as multireference. Second, a large basis is needed to capture excitations involving non-valence orbitals; for example, the formation of the 3d-3d bonds requires the 3p electrons to move out of the same spatial region by exciting to higher lying orbitals; such effects are referred to as dynamic correlation. The problem is computationally challenging because both the static and dynamic correlation must be computed sufficiently well even for a qualitatively reasonable description. For example, the valence complete active space self-consistent-field method (which treats the valence static correlation exactly but neglects the dynamic correlation) does not yield a minimum near the equilibrium bond length,<sup>21</sup> while the gold-standard treatment of dynamical correlation, coupled cluster singles, doubles and perturbative triples (CCSD(T)) also does not yield a reasonable bond length, nor does it display a shelf region.<sup>22</sup>

Figure 1 shows curves from calculations over many years; the lack of consensus is striking. Even when limited to studies from the last decade, there is a spread of over 0.6 eV in the predicted binding energy and 0.2 – 0.34 eV across the whole curve. Experimentally, while multiple techniques have shed light on the spectroscopic constants, information on the full PEC comes from a photoelectron spectroscopy study of Cr<sub>2</sub><sup>-</sup>.<sup>10,11</sup> This measured 29 vibrationally resolved transitions, and by assigning these to specific vibrational quantum numbers *v*, a PEC was derived using the Rydberg-Klein-Rees method. However, the assignments above *v* = 9 are uncertain, in particular, the assignment of the starting quantum number *v*<sub>prog</sub> of a high-lying 20 member vibrational progression. Together with non-uniqueness in the PEC fit, this leads to considerable uncertainty in the experimental PEC. This is shown by the shaded region of Figure 2a, which shows the range of experimental PEC arising from different assignments (*v*<sub>prog</sub> = 21 – 25), all of which match the observed vibrational levels within their experimental uncertainty; in the shelf-region the uncertainty is over 0.1 eV. (Further details in the SI).

To compute a more accurate PEC, we will employ a composite method starting from the scalar relativistic “exact two-component” (X2C) Hamiltonian,<sup>23,24</sup> which is based on two contributions. The first contribution estimates the exact chromium dimer PEC in a moderate basis (Dunning’s cc-pVDZ-DK basis, here dubbed PDZ,<sup>25</sup> with a frozen neon core, correlating 28 electrons in 76 orbitals). For this, we use data from very large ab initio density matrix renormalization group (DMRG) calculations (using up to bond dimension 28000 and SU(2) symmetry), together with selected heat-

bath configuration interaction (SHCI) data computed earlier by one of us.<sup>26</sup> The second contribution targets the remaining dynamic correlation. For this, we use data computed from multi-reference perturbation theory (using an efficient formulation of the restraining the excitation-order Hamiltonian<sup>27,28</sup> within the language of matrix product state perturbation theory,<sup>28–30</sup> starting from the 12 electron, 12 orbital valence complete active space) computed using cc-pVNZ-DK basis sets up to quintuple zeta, as well as unrestricted CCSD(T) data.<sup>26</sup> This dynamical correlation correction is then extrapolated to the basis set limit. We perform the simulations with the PySCF and block2 program packages.<sup>30–33</sup>

It is important to estimate the error in these various contributions. For the PDZ curve, as DMRG and SHCI provide independent extrapolations to numerical exactness with similar confidence, we take the average of the DMRG and SHCI data as the curve, with half the difference as the error ( $\epsilon_{\text{PDZ}}$ ). For the dynamic correlation correction, the CCSD(T) data is expected to be less accurate than the REPT data, due to the multireference nature of the correlation. Thus we only use the REPT data, and use half the difference from CCSD(T) as the error ( $\epsilon_{\text{REPT}}$ ). Finally, the basis set error is estimated as the standard deviation of the complete basis set (CBS) extrapolation fit ( $\epsilon_{\text{CBS}}$ ). Taking these three error contributions as independent, the total error is then the square root of the quadratic sum. Note that it is difficult to assert the statistical significance of these error estimates, however, they provide a useful measure of accuracy.

Using the new theoretical PEC, we compute the detailed vibrational spectrum by solving the vibrational Schrödinger equation. We use this to then reassign the measured experimental peaks from the photoelectron spectrum,<sup>11</sup> and with these assignments, solve the inverse Schrödinger equation to derive a new experimental PEC.

We show the computed PEC in Figure 2a. The accompanying error estimates for the PDZ curve, the dynamic correlation correction, and the CBS extrapolation are shown in Figure 2b.  $\epsilon_{\text{PDZ}}$  is quite small  $< 0.01$  eV, demonstrating remarkable agreement in the “exact” PDZ energies from DMRG and SHCI.  $\epsilon_{\text{CBS}}$  is also small  $< 0.012$  eV. The largest error is from the dynamic correlation which is as large as  $\sim 0.034$  eV at  $\sim 2.0$ – $2.25$  Å. As discussed in the SI, this likely reflects the poor performance of the CCSD(T) method used to estimate the error, and thus this large error is a conservative estimate (other ways of estimation given in the SI). Overall, we find good agreement with the existing experimental PEC, and one that is significantly improved over all previous computations in the literature (the next best match is shown in Figure 2c, which has substantial disagreement in the shelf region). Unlike some earlier predictions, no double minimum is observed. The largest uncertainties in the theoretical curve lie outside of the region of the PEC with large experimental uncertainty; we return to this point below.

Figure 3 shows spectroscopic constants derived from the current and earlier PECs, compared to experiment. We find very good agreement with experiment; the improvement in theoretical predictions over time is shown in the lowest panel. Note, however, that the spectroscopic constants only measure the quality of the PEC only near the minimum. In fact, the other studies with spectroscopic constants with small mean error are associated with PECs of poor overall shape (see Figure 1), reflecting a poor description of the full vibrational spectrum.

We now more carefully examine the shelf region of the

PEC, where there is the largest deviation from the experimentally derived curve. Ref. 11 contains a progression of 20 vibrational levels starting from  $4880$   $\text{cm}^{-1}$ , with a spacing of approximately  $128$   $\text{cm}^{-1}$ . Casey and Leopold tried various assignments, ultimately assigning the first frequency of this cluster to  $v_{\text{prog}} = 24$ . The vibrational frequencies for our theoretical PEC are shown in Figure 4a. With the old assignment of  $v_{\text{prog}}$ , our simulated frequencies of this cluster consistently disagree with the experimental result by approximately a single energy quantum in the shoulder region of the PEC (Figure 4b). This is surprising given the small theoretical estimate of the error in this region, and suggests that we should simply change the assignment from  $v_{\text{prog}} = 24$  to  $v_{\text{prog}} = 23$ . This reduces the root mean square deviation (RMSD) from  $113$   $\text{cm}^{-1}$  to  $19$   $\text{cm}^{-1}$ . The largest discrepancy now occurs for one of the lower states ( $v = 7$ ), consistent with the region of largest uncertainty in the theoretical calculations, between  $2.0$ – $2.25$  Å, (see Figure 4b). Notably, the experimental vibrational frequencies have a RMSD of  $16$   $\text{cm}^{-1}$ , similar to the RMSD of the computed frequencies with the new assignment. (See Table S4 in the SI). While theory does not allow for a statistical estimate of certainty, the quantitative agreement between the theoretical and experimental vibrational frequencies across the measured peaks is striking and is our main result. As a consequence, solving the inverse Schrödinger equation with the suggested new assignment of  $v_{\text{prog}}$  leads to a revised estimate of the experimental PEC shown in Figure 2a. The revised PEC demonstrates an excellent match between theory and experiment.

The computational prediction of the ground-state PEC of a diatomic that is quantitatively consistent with experiment might seem to be a standard task, but in the case of the chromium dimer it has been a challenge for decades. Our work shows that this goal can finally be achieved; as one metric, the average error in the vibrational spectrum computed from the theoretical PEC is now comparable to the average uncertainty of the vibrational peaks measured in experiment. While this arguably brings to a close a storied problem of computational quantum chemistry, it opens the door to many others, in particular, the applications of the theoretical techniques discussed here not only to other complex multiple metal-metal bonded species, but more generally to the quantitative spectroscopic modeling of transition metal clusters.

**Acknowledgement** We thank Doreen Leopold and Alec Wodtke for helpful discussions. Work by G.K.C. was supported by the US National Science Foundation (NSF) via grant no. CHE-2102505. G.K.C. acknowledges additional support from the Simons Foundation via the Many-Electron Collaboration and the Investigator Award. Work by H.R.L., H.Z. and C.J.U. was supported by the Air Force Office of Scientific Research, under Award FA9550-18-1-0095. H.R.L. acknowledges support from a postdoctoral fellowship from the German Research Foundation (DFG) via grant LA 4442/1-1 during the first part of this work. Some of the computations were conducted at the Resnick High Performance Computing Center, a facility supported by the Resnick Sustainability Institute at the California Institute of Technology. The SHCI calculations were performed on the Bridges computer at the Pittsburgh Supercomputing Center under grant PHY170037.

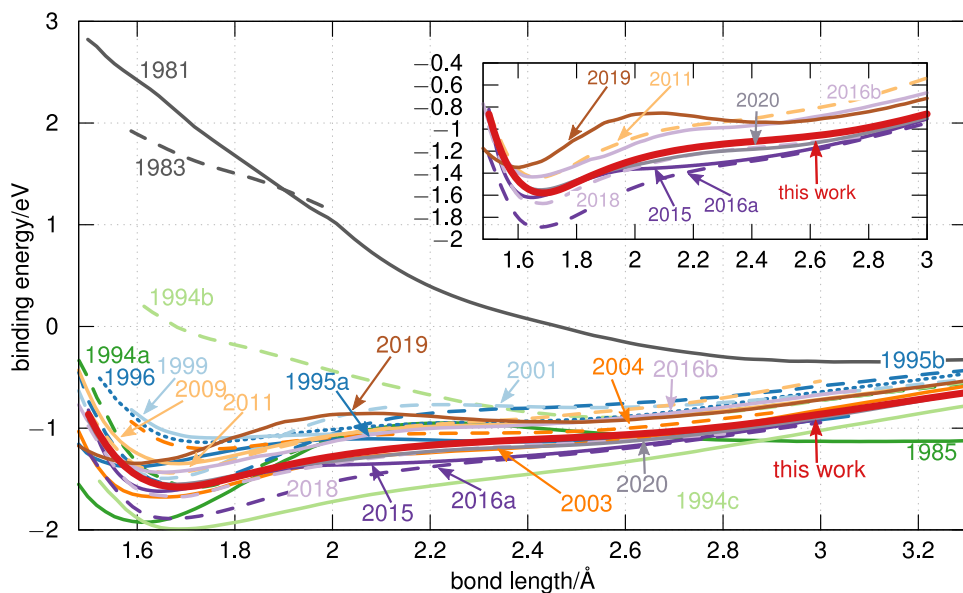


**Figure 1.** Some of the simulated potential energy curves (PECs) of the chromium dimer available in the literature, labeled by year. The red curve marks this work. The inset shows selected PECs from 2011 onwards.

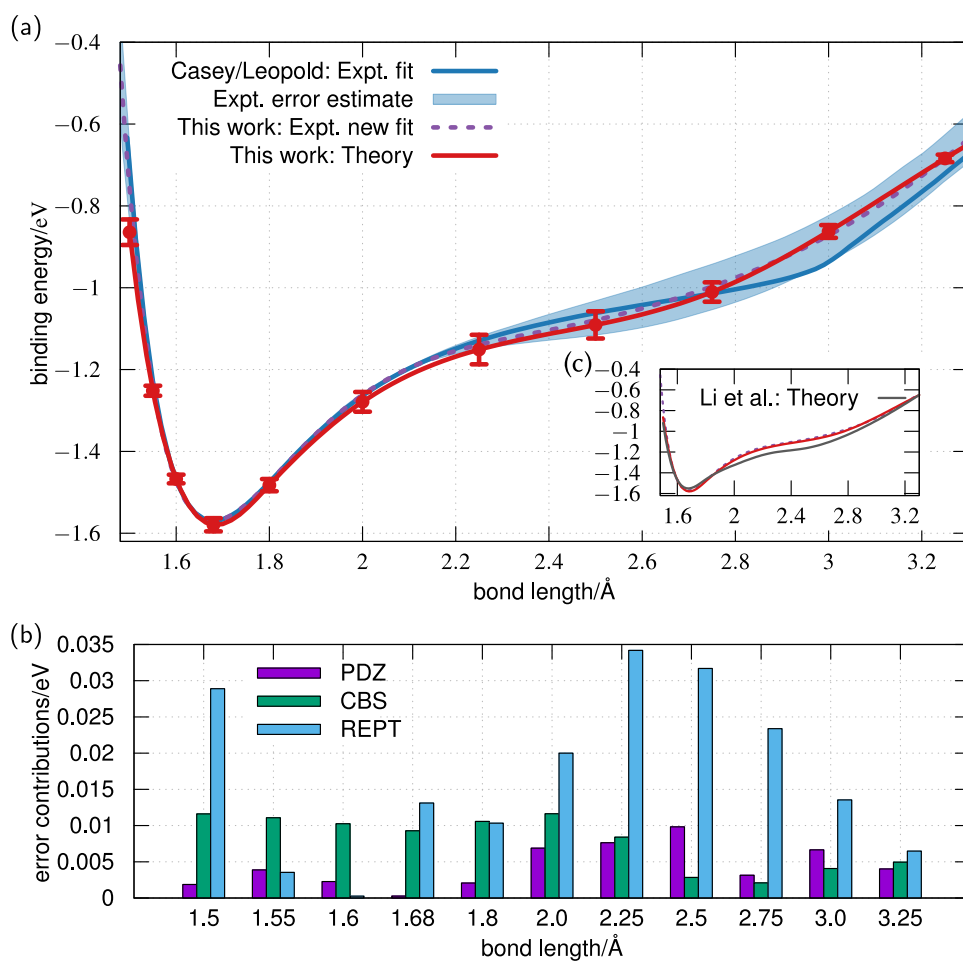


**Figure 2.** Theoretical and experimental potential energy curves (PECs) of the chromium dimer. (a) Blue: experimental PEC from Ref. 11. The blue-shaded area estimates the uncertainty from the experimental PEC fit. Purple: new experimental PEC from vibrational assignment in this work. Red: computed PEC with error estimates. (b) Estimated simulation errors.  $\epsilon_{\text{PDZ}}$ : error of “exact” estimate of the cc-pVDZ-DK basis curve.  $\epsilon_{\text{CBS}}$ : error in the complete basis-set extrapolation.  $\epsilon_{\text{REPT}}$ : error of the dynamic correlation correction. (c) New theoretical and experimental PEC compared with the next best PEC in the literature from Li et al. (gray curve).<sup>26</sup>

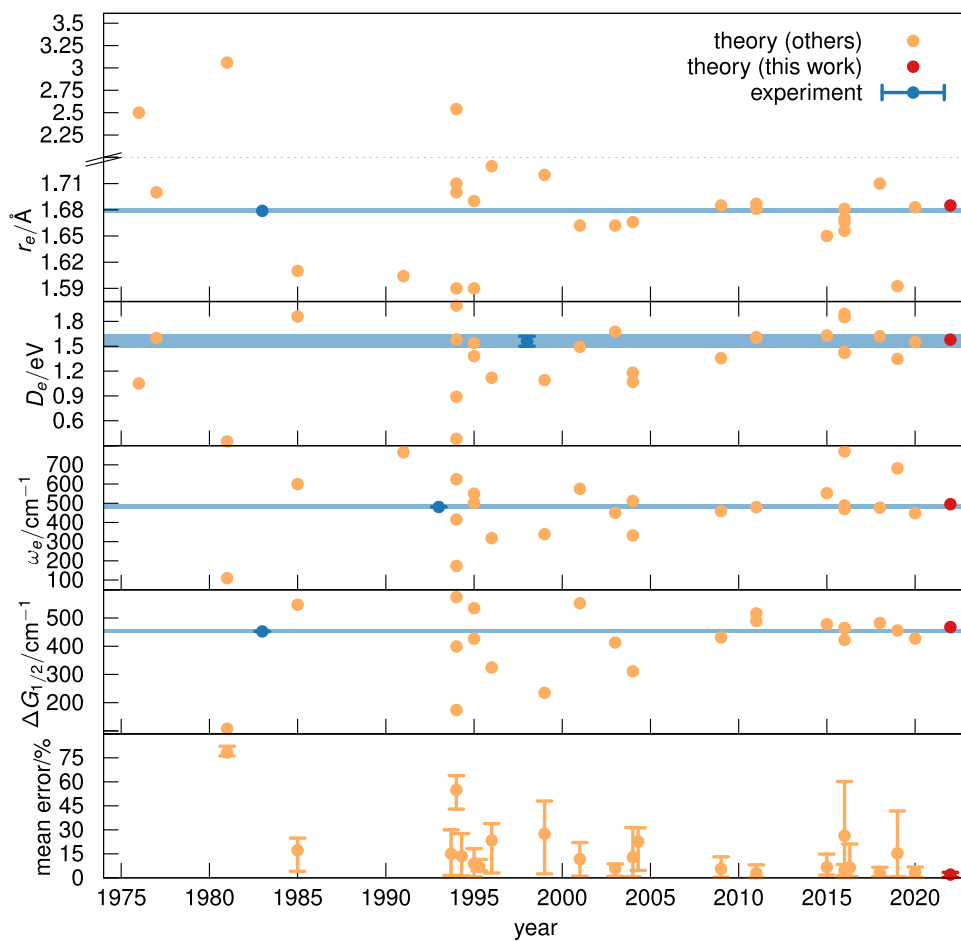


**Figure 3.** Simulated spectroscopic constants of  $\text{Cr}_2$  over time:  $r_e$  (equilibrium bond length),  $D_e$  (well-depth),  $\omega_e$  (harmonic frequency) and  $\Delta G_{1/2}$  (fundamental frequency). Blue: most recent experimental result; shaded area: experimental uncertainty (that of  $r_e$  is not reported). The lowest panel shows the evolution of the average absolute percentage error (in case all four constants are available; error bar shows min/max error). Further data is shown in the SI (Table S5).

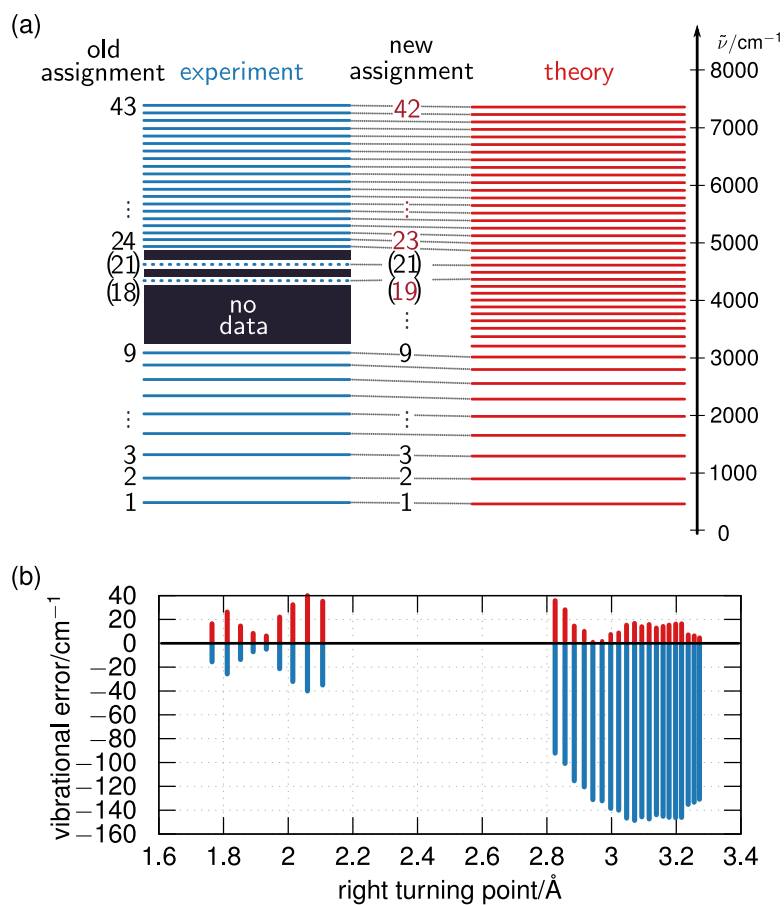


**Figure 4.** Vibrational ladder (a): Experimental (left) vibrational frequencies compared with the simulated frequencies (right). The experimental data lacks values between  $\sim 3250 \text{ cm}^{-1}$  and  $\sim 4750 \text{ cm}^{-1}$ ; the original assignment of frequencies with quantum numbers larger than 9 is not fully certain. (Note that the two measured frequencies labeled in brackets have not definitively been associated with the  $\text{Cr}_2$  ground state, see Ref. 11). The simulated frequencies enable a new assignment, shown in red. (b): Vibrational error of the new (old) assignment shown as positive (negative) values, as function of the right classical turning point of each state (based on our new experimental PEC). For the 9 lowest vibrational levels, associated with turning points up to  $2.1 \text{ \AA}$ , the assignment does not change and the errors are identical. For the 20 higher-lying levels, the old (new) assignment uses  $v_{\text{prog}} = 24(23)$ .

**Data Availability** Data for reproducing Figure 2a is available at <https://github.com/h-larsson/Cr2Pes22>. Further data is available from the authors upon reasonable request.

## Supporting Information Available

See Supplementary Information (SI) for additional details on the electronic structure methods (Section S1), the vibrational spectrum (S2), the PEC fit (S3), the assignment (S4), the uncertainty estimate of the experimental PEC (S5), as well as references for Figure 1 (S6).

### References

- (1) Kurashige, Y.; Chan, G. K.-L.; Yanai, T. Entangled Quantum Electronic Wavefunctions of the  $\text{Mn}_4\text{CaO}_5$  Cluster in Photosystem II. *Nat. Chem.* **2013**, *5*, 660–666.
- (2) Sharma, S.; Sivalingam, K.; Neese, F.; Chan, G. K.-L. Low-Energy Spectrum of Iron–sulfur Clusters Directly from Many-Particle Quantum Mechanics. *Nat. Chem.* **2014**, *6*, 927–933.
- (3) Li, Z.; Guo, S.; Sun, Q.; Chan, G. K.-L. Electronic landscape of the P-cluster of nitrogenase as revealed through many-electron quantum wavefunction simulations. *Nat. Chem.* **2019**, *11*, 1026–1033.
- (4) Klotzbuecher, W.; Ozin, G. A.; Norman, J. G.; Kolari, H. J. Bimetal Atom Chemistry. 1. Synthesis, Electronic Absorption Spectrum, and Extended Hueckel/Self-Consistent Field-X $\alpha$ -Scattered Wave Molecular Orbital Analyses of the Chromium-Molybdenum (CrMo) Molecule: Relevance to Alloy and Bimetallic Cluster Catalysis. *Inorg. Chem.* **1977**, *16*, 2871–2877.
- (5) Cotton, F. A. Discovering and Understanding Multiple Metal-to-Metal Bonds. *Acc. Chem. Res.* **1978**, *11*, 225–232.
- (6) Goodgame, M. M.; Goddard, W. A. The "Sextuple" Bond of Chromium Dimer. *J. Phys. Chem.* **1981**, *85*, 215–217.
- (7) Goodgame, M. M.; Goddard, W. A. Modified Generalized Valence-Bond Method: A Simple Correction for the Electron Correlation Missing in Generalized Valence-Bond Wave Functions; Prediction of Double-Well States for  $\text{Cr}_2$  and  $\text{Mo}_2$ . *Phys. Rev. Lett.* **1985**, *54*, 661–664.
- (8) Bondybey, V. E.; English, J. H. Electronic Structure and Vibrational Frequency of  $\text{Cr}_2$ . *Chem. Phys. Lett.* **1983**, *94*, 443–447.
- (9) Anderson, A. B. Structures, Binding Energies, and Charge Distributions for Two to Six Atom Ti, Cr, Fe, and Ni Clusters and Their Relationship to Nucleation and Cluster Catalysis. *J. Chem. Phys.* **1976**, *64*, 4046–4055.
- (10) Casey, S. M.; Villalta, P. W.; Bengali, A. A.; Cheng, C. L.; Dick, J. P.; Fenn, P. T.; Leopold, D. G. A Study of Chromium Dimer ( $\text{Cr}_2$ ) by Negative-Ion Photoelectron Spectroscopy. *J. Am. Chem. Soc.* **1991**, *113*, 6688–6689.
- (11) Casey, S. M.; Leopold, D. G. Negative Ion Photoelectron Spectroscopy of Chromium Dimer. *J. Phys. Chem.* **1993**, *97*, 816–830.
- (12) Thomas, E. J.; Murray, J. S.; O'Connor, C. J.; Politzer, P. The  $\text{Cr}_2$  Molecule: Some Perspectives. *J. Mol. Struct-THEOCHEM* **1999**, *487*, 177–182.
- (13) Roos, B. O. The Ground State Potential for the Chromium Dimer Revisited. *Collect. Czech. Chem. Commun.* **2003**, *68*, 265–274.
- (14) Roos, B. O.; Borin, A. C.; Gagliardi, L. Reaching the Maximum Multiplicity of the Covalent Chemical Bond. *Angew. Chem. Int. Ed.* **2007**, *46*, 1469–1472.
- (15) Li Manni, G.; Ma, D.; Aquilante, F.; Olsen, J.; Gagliardi, L. SplitGAS Method for Strong Correlation and the Challenging Case of  $\text{Cr}_2$ . *J. Chem. Theory Comput.* **2013**, *9*, 3375–3384.
- (16) Brynda, M.; Gagliardi, L.; Widmark, P.-O.; Power, P. P.; Roos, B. O. A Quantum Chemical Study of the Quintuple Bond between Two Chromium Centers in  $[\text{PhCrCrPh}]$ : Trans-Bent versus Linear Geometry. *Angew. Chem. Int. Ed.* **2006**, *45*, 3804–3807.
- (17) Wagner, F. R.; Noor, A.; Kempe, R. Ultrashort metal–metal distances and extreme bond orders. *Nature Chem.* **2009**, *1*, 529–536.
- (18) Stein, C. J.; Pantazis, D. A.; Krewald, V. Orbital Entanglement Analysis of Exchange-Coupled Systems. *J. Phys. Chem. Lett.* **2019**, 6762–6770.
- (19) Chalupský, J.; Srnc, M.; Yanai, T. Interpretation of Exchange Interaction through Orbital Entanglement. *J. Phys. Chem. Lett.* **2021**, *12*, 1268–1274.
- (20) Nguyen, T.; Sutton, A. D.; Brynda, M.; Fetting, J. C.; Long, G. J.; Power, P. P. Synthesis of a Stable Compound with Fivefold Bonding Between Two Chromium(I) Centers. *Science* **2005**, *310*, 844–847.
- (21) Walch, P.; Bauschlicher, C. W.; Roos, Björn O.; Nelin, Constance J., Theoretical evidence for multiple 3D bonding in the  $\text{V}_2$  and  $\text{Cr}_2$  molecules. *Chem. Phys. Lett.* **1983**, *103*, 5.
- (22) Bauschlicher, C. W.; Partridge, H.  $\text{Cr}_2$  Revisited. *Chem. Phys. Lett.* **1994**, *231*, 277–282.
- (23) Peng, D.; Reiher, M. Exact Decoupling of the Relativistic Fock Operator. *Theor. Chem. Acc.* **2012**, *131*, 1081.
- (24) Kutzelnigg, W.; Liu, W. Quasirelativistic Theory Equivalent to Fully Relativistic Theory. *J. Chem. Phys.* **2005**, *123*, 241102.
- (25) Balabanov, N. B.; Peterson, K. A. Systematically Convergent Basis Sets for Transition Metals. I. All-Electron Correlation Consistent Basis Sets for the 3d Elements Sc–Zn. *J. Chem. Phys.* **2005**, *123*, 064107.
- (26) Li, J.; Yao, Y.; Holmes, A. A.; Otten, M.; Sun, Q.; Sharma, S.; Umrigar, C. J. Accurate many-body electronic structure near the basis set limit: Application to the chromium dimer. *Phys. Rev. Research* **2020**, *2*, 012015.
- (27) Fink, R. F. The multi-reference retaining the excitation degree perturbation theory: A size-consistent, unitary invariant, and rapidly convergent wavefunction based ab initio approach. *Chem. Phys.* **2009**, *356*, 39–46.
- (28) Sharma, S.; Alavi, A. Multireference linearized coupled cluster theory for strongly correlated systems using matrix product states. *J. Chem. Phys.* **2015**, *143*, 102815.
- (29) Sharma, S.; Chan, G. K.-L. Communication: A flexible multi-reference perturbation theory by minimizing the Hylleraas functional with matrix product states. *J. Chem. Phys.* **2014**, *141*, 111101.
- (30) Larsson, H. R.; Zhai, H.; Gunst, K.; Chan, G. K.-L. Matrix Product States with Large Sites. *J. Chem. Theory Comput.* **2022**, *18*, 749–762.
- (31) Sun, Q.; Berkelbach, T. C.; Blunt, N. S.; Booth, G. H.; Guo, S.; Li, Z.; Liu, J.; McClain, J. D.; Sayfutyarova, E. R.; Sharma, S.; Wouters, S.; Chan, G. K. PySCF: the Python-based simulations of chemistry framework. *WIREs Comput Mol Sci* **2017**, *8*, e1340.
- (32) Sun, Q. et al. Recent developments in the PySCF program package. *J. Chem. Phys.* **2020**, *153*, 024109.
- (33) Zhai, H.; Chan, G. K.-L. Low Communication High Performance Ab Initio Density Matrix Renormalization Group Algorithms. *J. Chem. Phys.* **2021**, *154*, 224116.